RESEARCH Revista Mexicana de Física **59** (2013) 148–152 MARCH–APRIL 2013

Microwave noise sources contributions to SiGe:C/Si and InP/InGaAs HBT's performances

A. Pacheco-Sánchez[a], E. Ramírez-García[a], L. Rodríguez-Méndez[a], M.Galaz-Larios[a],
C. Márquez-Beltrán[b], and M. Enciso-Aguilar[a]

[a] *Instituto Politécnico Nacional, Escuela Superior de Ingeniería Mecánica y Eléctrica,*
Unidad Profesional "Adolfo López Mateo". Edif. Z-4 3er. Piso 07738, D.F. México,
Sección de Estudios de Posgrado e Investigación, Maestría en Ciencias en Ingeniería de Telecomunicaciones,
e-mail: mencisoa@ipn.mx; anibalverbeno@gmail.com

[b] *Instituto de Física, Benemérita Universidad Autónoma de Puebla,*
Apartado Postal J-48, Puebla 72570, México.

Received 8 May 2012; accepted 12 November 2012

The present work describes the quantification of the noise sources contributions to the microwave transistor noise performance, particularly focusing on the minimum noise factor (F_{min}) and on the equivalent noise resistance (R_n). For this analysis microwave noise small-signal modeling is used. This study is performed for one SiGe:C/Si and one InP/InGaAs heterojunction bipolar transistor (HBT) at several bias points and at two operation frequencies. It is shown that some parameters usually neglected to develop simplified formulas for noise analysis have a non-negligible contribution to F_{min} and R_n. This demonstrates that for other HBT technologies it is necessary to carry out a similar study in order to determine whether noise sources can be neglected or not. This procedure may be useful when deriving simplified and accurate models of microwave noise analysis. The development of accurate and simplified analytical models for noise analysis for many other HBT (III-V and IV-IV) technologies may benefit from this procedure.

Keywords: Emitter resistance; heterojunction bipolar transistor; microwave noise; small-signal noise modeling.

En este trabajo se describe la cuantificación de las diferentes fuentes de ruido que contribuyen al funcionamiento en ruido del transistor, orientándose particularmente sobre el factor de ruido mínimo (F_{min}) y la resistencia de ruido equivalente (R_n), para ello nos basamos en el modelado en pequeña señal de altas frecuencias con ayuda del circuito eléctrico equivalente. El análisis es llevado a cabo para dos transistores bipolares de heterounión (TBH), uno SiGe:C y otro InP/InGaAs. Este estudio es realizado bajo diferentes niveles de polarización y para dos frecuencias de operación. Los resultados muestran que algunos parámetros usualmente despreciados para el análisis de ruido de microondas tienen una contribución no despreciable sobre F_{min} y R_n. Esto es un indicador de que es necesario realizar un estudio similar al descrito en este artículo para determinar si una fuente de ruido puede ser despreciada o no. Este procedimiento puede ser aplicado para el desarrollo de modelos de análisis de ruido microondas simplificados y precisos que podrían ser útiles para una gran gama de TBH (III-V and IV-IV).

Descriptores: Modelado eléctrico de ruido; resistencia de emisor; ruido de microondas; transistor bipolar de heterounión.

PACS: 07.50.Hp; 85.30.De; 85.30.Pq; 85.40.Qx

1. Introduction

SiGe heterojuntion bipolar transistors (HBT) are the backbone of BiCMOS technology. In the near future this device will be the key device for development of radio frequency (RF), microwave and optical applications. At room temperature state-of-the-art SiGe HBTs reach unitary current gain (f_T) and maximum oscillation frequencies (f_{MAX}) in excess of 500 GHz [1-3]. These impressive dynamic performances are achieved because of device conception improvements, see [1-3] for further details. Dynamic performances of InP/InGaAs HBTs are even higher than those of the SiGe HBTs. f_T and f_{MAX} in excess of 750 GHz at room temperature have been achieved many years ago [4-5]. However, the technology of these last devices has two drawbacks: (a) III-V HBT technology is not as mature as Si-based technology and (b) III-V HBT technology is more expensive than Si-based technology. Moreover, no industrial applications of such HBTs have been reported until now.

When a semiconductor device is used as an amplifier it is desirable that it adds the lowest noise level as possible [6]. HBTs have achieved excellent noise performance, *e.g.* in Ref. 7 an InP/InGaAs HBT with an NF_{min} of 0.6 dB at 2 GHz is reported. Further, an excellent low noise performance is achieved for the SiGe HBT described in Ref. 8, with an NF_{min} as low as 0.4 dB at 10 GHz.

These excellent dynamic and microwave noise (μWN) performances of IV-IV and III-V HBTs make them serious contenders for the development of ultra-high speed and very low noise applications.

μWN modeling, electrical or physical, is a fundamental tool in the electronics industry because it helps to identify, quantify and optimize the different elements that contribute to noise in semiconductor devices [6]. A microscopic analysis of μWN must consider heat and carrier transport within a realistic HBT structure. However, the numerical modeling required to address this problem is quite complex and is outside the scope of this paper. In contrast, small-signal

electrical modeling represents a fast, simple and reliable alternative to quantify the different source contributions to the overall device noise performance. It is well known that the noise performance of any active device is characterized by the minimum noise factor (F_{min}), the equivalent noise resistance (R_n) and the optimum admittance (Y_{opt}) [9]. In the framework of the small-signal equivalent circuit model, μWN is modeled by the thermal noise produced by the access parasitic resistances of the HBT and by the shot-noise produced by the random injection of carriers at the junctions of the bipolar devices.

An important but rarely addressed topic is the elucidation of the noise source contribution to F_{min} and R_n. To the authors' knowledge this type of study has not been reported yet on HBT devices. Hence, in this work, the weight of the different noise sources contributions to F_{min} and R_n is reported. Furthermore, we demonstrate that in order to develop simplified formulas for noise analysis the commonly neglected elements must be included as they have a non-negligible influence over F_{min} and/or R_n. F_{min} and R_n parameters are addressed because they give more insight into the physics of the device noise performance than Y_{opt}.

Section 2 introduces the device description and the small-signal equivalent circuit used for the device noise modeling. Section 3 analyzes and discusses the results.

2. Device Description and The Small-Signal Model

To perform the task of modeling, the small-signal equivalent circuit elements are extracted from S-parameters measurements for the HBT devices reported in Ref. 10. Briefly, for the SiGe:C device the Ge fraction of the 30 nm thick base is gradual varying from 10% to 30% from emitter to collector side. The emitter surface (S_E) is equal to 0.17 × 5.7 μm^2.

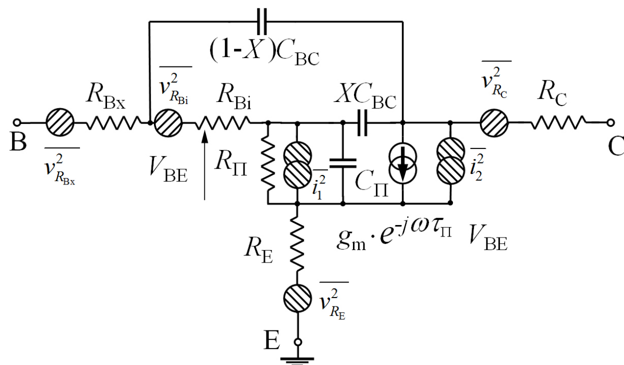

FIGURE 1. Small-signal Π-equivalent circuit of the HBTs including thermal and shot noise sources; see the text for their definition. R_{E}, R_{C}, R_{Bx} and R_{Bi} are, respectively, the emitter, the collector, the extrinsic and intrinsic base resistances. X is the distribution factor between the apparent base resistance (R_{B}) and the base collector capacitance (C_{BC}) [14]. The other parameters (R_{Π}, g$_m$, τ_{Π} and C_{Π}) have their standard meaning [16].

TABLE I. Electrical parameters of the Π-equivalent circuit shown in Fig. 1. for both HBTs.

Bias independent elements [10]		
Element	SiGe HBT	InP HBT
R_{Bx} (Ω)	15.5	9.7
R_{E} (Ω)	8.9	3.8
R_{C} (Ω)	5.0	2.0
Bias dependent elements		
Element	$J_{\text{C1,SiGe}}/J_{\text{C2,SiGe}}$ 3.0/9.78 (mA/μm^2)	$J_{\text{C1,InP}}/J_{\text{C2,InP}}$ 1.9/5.5 (mA/μm^2)
R_{Π} (kΩ)	7.3/0.96	0.41/0.026
R_{Bi} (Ω)	30.5/20.0	16.5/7.3
C_{Π} (fF)	58/210	80/390
C_{BC} (fF)	6.4/6.9	10.1/11
$X C_{\text{BC}}$ (fF)	3.5/1.2	3.4/3.5
g_m (mS)	91/360	42.5/950

Further details concerning the device conception are described in Ref. 11. The InP/InGaAs double HBT, hereafter called InP HBT is developed by Alcatel-Thales III-V Lab. The HBT structure includes a 28 nm thick highly carbon doped and compositionally graded base, with $S_E = 0.7 \times 10$ μm^2. More details about the device conception are found in Ref. 12.

Figure 1 shows the small-signal Π-equivalent circuit, including the associated thermal noise sources to each resistor and the non-correlated shot noise sources between base-emitter (BE) and base-collector (BC) junctions; the values of each parameter are listed in Table I. Excellent agreement between the model and measurements (μWN and S-parameters) is demonstrated for both HBTs [10]. The small-signal equivalent circuit depicted in Fig. 1 was implemented on the commercially available software Advanced Design System from Agilent to obtain both μWN performance and S-parameters.

Some parameters of the bipolar transistor small-signal Π-equivalent circuit were extracted by means of analytical-based methods [13]. R_{E} was obtained from the extrapolation of the real part of Z_{12} at infinite current. The apparent base resistance (R_{B}) was derived from the real part of Z_{11}–Z_{12} parameters, and the total C_{BC} was extracted from the imaginary part of Z_{22}–Z_{21}. The remaining parameters of the Ï-equivalent circuit ($R_{\ddot{I}}$, g_m, $C_{\ddot{I}}$) were obtained by a minimization procedure of the difference between measured and simulated S-parameters; the Π time delay ($\tau_{\ddot{I}}$) was found to be negligible at all bias levels for both HBTs. The collector distribution factor (X) acts on R_{B} as a capacitive bridge, *i.e.*, $R_{\text{B}} = R_{\text{Bx}} + X R_{\text{Bi}}$ [14]. This means that this parameter splits the total BC capacitance (C_{BC}) in two parts, as can be seen in Fig. 1. X was extracted by a minimization procedure to match modeled and measured noise parameters [15].

The expressions for thermal and non-correlated shot noise sources are, respectively, given by

$$\overline{v_{\mathrm{R}_i}^2} = 4k_{\mathrm{B}}T_R R_i$$

and

$$\overline{i_{\mathrm{B,C}}^2} = 2qI_{\mathrm{B,C}},$$

where k_{B} is the Boltzmann constant, R_i is the corresponding HBT access resistance, q is the electron charge, $I_{\mathrm{B,C}}$ stands for the DC base or collector current, and T is the effective temperature of the access resistances.

T takes into account self-heating (SH) in the HBTs, and this parameter is computed as: $T = T_{\mathrm{room}} + P_D R_{\mathrm{TH}}$, where T_{room} is the room temperature without SH (293 K), P_D ($= V_{\mathrm{CE}}I_{\mathrm{C}}$) is the electrical power dissipated by the device, and R_{TH} is the thermal resistance of each HBT. The procedure to extract R_{TH} is well described in [17,18]. For the SiGe HBT T is equal to 307 K at $J_{\mathrm{C1,SiGe}}$ and 340 K at $J_{\mathrm{C2,SiGe}}$. For the InP HBT T is equal to 380 K and 517 K at $J_{\mathrm{C1,InP}}$ and $J_{\mathrm{C2,InP}}$, respectively.

The next section presents the results of the contribution of each μWN source to F_{min} and R_n.

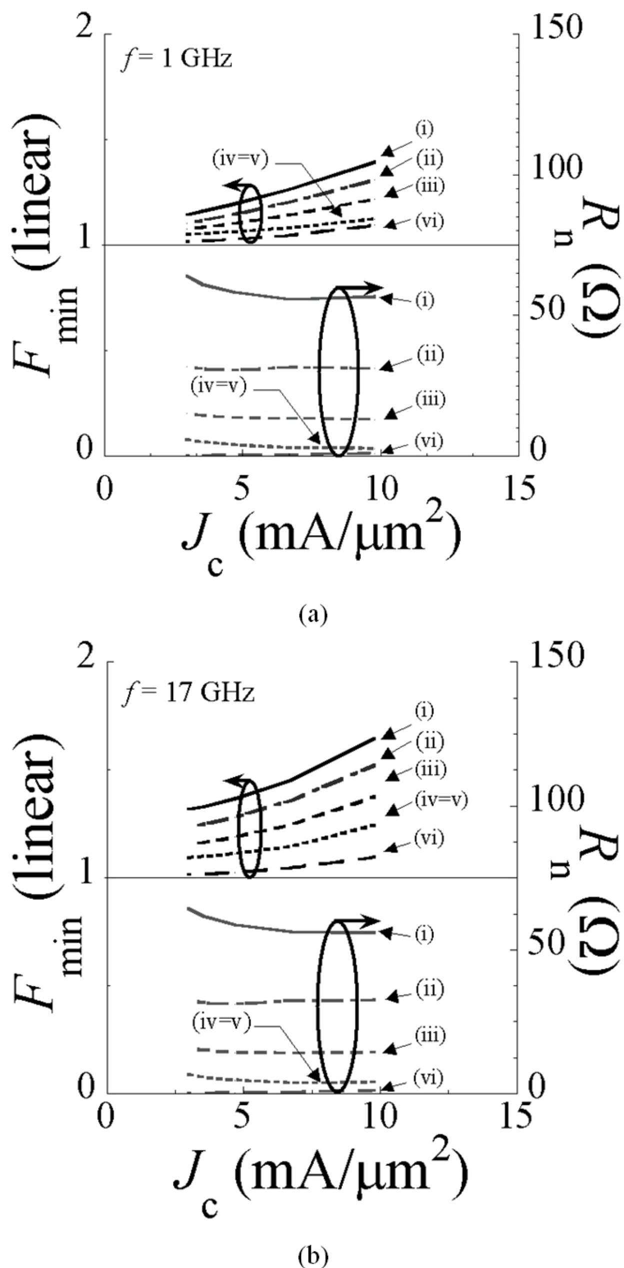

FIGURE 2. F_{min} and R_n as a function of current density for the SiGe HBT. (a) 1 GHz (b) 17 GHz. (i) all noise sources on; (ii) the noise source R_{Bi} off; (iii) noise sources R_{Bx} and R_{Bi} are off; (iv) noise sources R_{Bx}, R_{Bi} and RE are off; (v) noise sources RBx, R_{Bi}, RE and RC are off; (vi) noise sources R_{Bx}, R_{Bi}, R_{E}, R_C and i_{n2} are off.

3. Results and discussion

In order to quantify the contribution of each noise source on F_{min} and R_n, they are turned off one-by-one within the Π-model; then F_{min} and R_n are extracted at each step and at several bias levels. This procedure ends when only one active noise source is on. Fig. 2 shows the results for the SiGe HBT. Qualitatively and quantitatively the same behavior was found for the InP HBT (not shown here for briefness). The contribution of the different noise sources to F_{min} and R_n at one polarization bias point are presented in Table II.

Firstly, the impact of the different noise sources on $F_{\mathrm{min,SiGe}}$ is discussed. From Table II we observe that $R_{\mathrm{Bi,SiGe}}$ has the highest influence of all the electrical elements on $F_{\mathrm{min,SiGe}}$. Its weight represents about 35% at the two operation frequencies. The second most important contribution to $F_{\mathrm{min,SiGe}}$ is i_{n1} with 32/10% at 1/17 GHz. $R_{\mathrm{E,SiGe}}$ represents 17/19% of $F_{\mathrm{min,SiGe}}$ at the same operation frequencies. $i_{\mathrm{n2,SiGe}}$ contributes with 2.3/18.7%. We observe that the weight of $i_{\mathrm{n1,SiGe}}$ and $i_{\mathrm{n2,SiGe}}$ on $F_{\mathrm{min,SiGe}}$ evolves strongly with f. The underlying reason of this behavior is the variation of the amplitude of the current gain of the SiGe device ($|H_{21,\mathrm{SiGe}}|$). As a matter of fact, $|H_{21,\mathrm{SiGe}}|$ has a slope of –20 dB/dec in the frequency range between 1–17 GHz (not shown here). Hence, the contribution of shot noise sources will evolve strongly with f. The noise contribution of $R_{\mathrm{C,SiGe}}$ is practically negligible in the whole frequency range and for the two frequency points.

Concerning $F_{\mathrm{min,InP}}$, we observe from Table II that the element with the most important noise contribution is i_{n1} with almost 51/47% at 1/17 GHz. The second most important noise contribution is $R_{\mathrm{Bi,InP}}$ with 23/22% at the frequencies considered. $R_{\mathrm{Bx,InP}}$ represents 10% of $F_{\mathrm{min,InP}}$ at 1/17 GHz. $R_{\mathrm{E,SiGe}}$ has a weight of 7% to $F_{\mathrm{min,InP}}$ at the two frequencies of analysis. $i_{\mathrm{n2,InP}}$ contributes with 7/13% at 1/17 GHz. The noise contribution of $i_{\mathrm{n2,InP}}$ evolves moderately with f because the slope of $|H_{21,\mathrm{InP}}|$ is lower than –20 dB/dec in the reported frequency range (not shown). We note that the contribution of R_C to $F_{\mathrm{min,InP}}$ is practically negligible.

The impact of noise sources on $R_{\mathrm{n,SiGe}}$ is now analyzed. From table II we observe that R_{Bi} has the strongest influence over $R_{\mathrm{n,SiGe}}$ with 50% weight at the frequencies reported.

TABLE II. Contribution in percentage to $F_{\rm min}$ and R_n of each electrical element at 1 and 17 GHz. $J_{\rm C1,SiGe}$ = 3.0 mA/μm^2 and $J_{\rm C1,InP}$ = 1.9 mA/μm^2.

	SiGe HBT f 1/17 (GHz)		InP HBT f 1/17 (GHz)	
Element	$\%F_{\rm min}$	$\%R_{\rm n}$	$\%F_{\rm min}$	$\%R_{\rm n}$
$R_{\rm Bi}$	35/34.8	50.5/50	22.9/21.9	44.6/44
$R_{\rm Bx}$	13/16.6	25.6/25.5	10.1/10.1	26.2/25.9
$R_{\rm E}$	17.4/18.9	14.7/14.5	7.6/7.1	10.3/10
$R_{\rm C}$	$\approx 0.0/0.9$	$\approx 0/0$	$\approx 0/0.1$	$\approx 0/0$
$i_{\rm n1}$	32.3/9.9	0.3/0.3	51.7/47.2	12/11.8
$i_{\rm n2}$	2.3/18.7	8.8/9.8	7.7/13.5	6.9/8.5

The second most important contribution is given by $R_{\rm Bx,SiGe}$ with 25% at 1/17 GHz. $R_{\rm E,SiGe}$ contributes around 15% of the total weight at the same operation frequencies. $i_{\rm n2,SiGe}$ has an influence on $R_{\rm n,SiGe}$ of 9/10% at 1/17 GHz. $i_{\rm n1,SiGe}$ and $R_{\rm C,SiGe}$ have virtually no impact on $R_{\rm n,SiGe}$ at the frequencies of analysis.

For $R_{\rm n}$ of the InP device, Table II shows that the most important contribution to $R_{\rm n,InP}$ is given by $R_{\rm Bi,InP}$ with 45% at 1/17 GHz. $R_{\rm Bx,InP}$ contributes with 26% at the same operation frequencies. $i_{\rm n1,InP}$ gives 12% of the total $R_{\rm n,InP}$. $R_{\rm E,InP}$ has a non-negligible weight of 10% to the noise resistance. $R_{\rm C,InP}$ is the only element that has no contribution to $R_{\rm n,InP}$.

The unexpected result is that, for both technologies, $R_{\rm E}$ has a non-negligible influence on $F_{\rm min}$ and/or on $R_{\rm n}$ at all polarization levels and for the two operation frequencies considered. Investigations usually neglect the influence of $R_{\rm E}$ on the overall device noise performance, see for instance [6]. Moreover, in Ref. 6 $R_{\rm B}$ is not separated into intrinsic and extrinsic parts, and SH is neglected. This may be a drawback of previously reported simplified μWN models. Perhaps the SH, $R_{\rm E}$ contribution and the influence of X to noise was negligible in the SiGe HBT described in Ref. 6, but these points were not addressed.

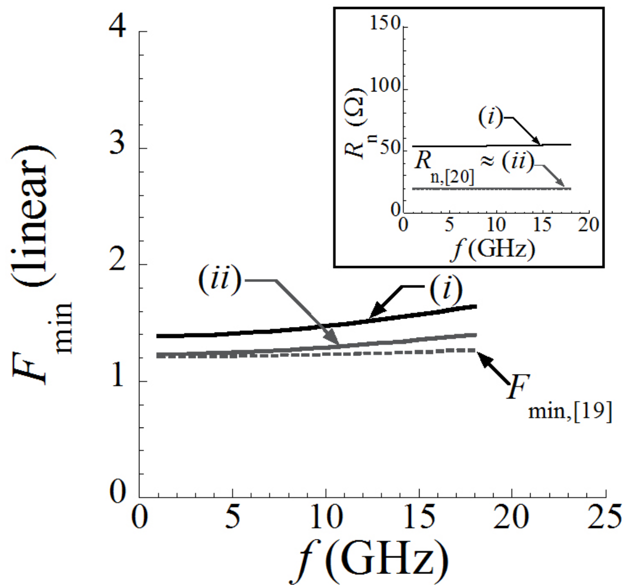

FIGURE 3. $F_{\rm min}$ and $R_{\rm n}$ (inset) as a function of frequency computed with formulas of references [19,20] and modeled for the SiGe HBT. Description of cases (i) and (ii) are provided in the text. $J_{\rm C}$ = 9.8 mA/μm^2, $V_{\rm CE}$ = 1.28 V

Figure 3 shows the comparison of computed $F_{\rm min}$ and $R_{\rm n}$ with the Π-model under the following conditions: (i) all the noise sources are switched on, the SH is turned on and X =0.1, and (ii) $R_{\rm E}$, and $R_{\rm C}$, are noiseless; SH is turned off, and X = 1, which means that $R_{\rm B}$ is not split into extrinsic and intrinsic parts. The computed values were derived using analytical formulas of Hawkins ($F_{\rm min}$) [19] and Pucel (R_n) [20]. The main simplifications of their work are identical to case (ii).

The comparison of computed and modeled $F_{\rm min}$ and $R_{\rm n}$ is discussed for the SiGe HBT only, because the same trend was found for the InP device at all bias levels and in the whole frequency range. Fig. 3 shows that $F_{{\rm min},(i)}$ and $R_{{\rm n},(i)}$ are higher than $F_{{\rm min},(ii)}$, $F_{\rm min,[19]}$, $R_{{\rm n},(ii)}$ and $R_{n,[20]}$, respectively. Another feature is that $F_{{\rm min},(ii)} \approx F_{\rm min,[19]}$ at operation frequencies $f < 10$ GHz. Similarly, Fig. 3 shows that $R_{{\rm n},(ii)} \approx R_{\rm n,[20]}$ in the whole frequency range. This behavior is not astonishing because, as already stated, $F_{{\rm min},(ii)}$, $F_{\rm min,[19]}$, $R_{{\rm n},(ii)}$ and $R_{\rm n,[20]}$ neglect the same parameters. Moreover, in Ref. 10 it was demonstrated that $F_{\rm min,[19]}$ and $R_{\rm n,[20]}$ severely underestimate measurements at all bias levels in the frequency range between 1–18 GHz.

These findings imply that before deriving simplified μWN models, it is necessary to evaluate the weight of the different noise sources contributions to $F_{\rm min}$ and R_n. For instance, if we want to derive accurate and simplified formulas of $F_{\rm min}$ and $R_{\rm n}$ for the two HBTs reported here, we can fairly neglect the influence of $R_{\rm C}$, while the remaining elements of the Π-equivalent circuit must be considered.

4. Conclusion

The contribution to $F_{\rm min}$ and R_n of the different noise sources contained in the Π-equivalent circuit of a SiGe and InP HBTs were quantified. The investigation was carried out at several bias levels and at two different operation frequencies. For the two HBT introduced in this work the noise contribution of $i_{\rm n1}$, $i_{\rm n2} R_{\rm E}$, $R_{\rm Bx}$, $R_{\rm Bi}$ and SH represent about the 99% of $F_{\rm min}$ and $R_{\rm n}$ at all bias levels and at the two frequencies highlighted. $R_{\rm C}$ is the only parameter that can be fairly neglected. This study contrasts with previous studies where to derive simplified formulas of noise analysis only $i_{\rm n1}$, $i_{\rm n2}$ and $R_{\rm B}$ (without separation into intrinsic and extrinsic parts) were considered. This indicates that in order to derive simplified and accurate models for μWN modeling of HBTs, it is necessary to perform a study to identify the main contributions to μWN.

Acknowledgements

We thank the Mexican National Council of Science and Technology (CONACyT-México) for the financial support under the contract no. 106698 and COFAA-IPN.

---

1. N. Zerounian, F. Aniel, B. Barbalat, P. Chevalier, and A. Chantre, *IET Electron Lett* **43** (2007) 1076-8.
2. N. Zerounian, E. Ramírez-García, F. Aniel, P. Chevallier, B. Geynet, and A. Chantre, *International SiGe & Ge: materials, processing, and device symposium of the joint international meeting of the 214th meeting of ECS*, (2008).
3. B. Heinemann *et al*., *Proc. of the (IEEE) International Electron Devices Meeting*, (December, 2010).
4. W. Snodgrass, W. Hafez, N. Harff, and M. Feng, *Proc. of IEDM (IEEE)* 2006).
5. E. Lobisser, Z. Griffith, Z. Jain, B. J. Thibeault, and M. Rodwell, *Proc. Indium Phosphide and Related Materials* (2009).
6. G. Niu, J. D. Cressler, S. Zhang, A. Joseph, and D. Harame, *Solid State Electronics* **46** (2002).
7. V. Danelon *et al*., *(IEEE) Microwave and Guided Wave Letters* **9** (1999).
8. D. R. Greenberg, B. Jagannathan, S. Sweeney, G. Freeman and D. Ahlgren, *Proc. IEDM* (IEEE Press 2002).
9. Haus *et al. Proc. of the IRE* **49** (1960).
10. E. Ramírez-García, F. Aniel, M. Enciso-Aguilar, and N. Zerounian, *submitted to Semiconductor Sicence and Technology*.
11. P. Chevalier *et al*., *Journal of Solid-State Circs.* **40** (2005).
12. J. Godin *et al*., "*Submicron InP DHBT technology for high speed high-swing mixed-signal ICs*", (Proc. of Compound Semiconductor Integrated Circuits Symposium, Oct 12–15, 2008).
13. A. Ouslimani, J. Gaubert, H. Hafdallah, A. Birafane, P. Pouvil and H. Leier, *Transactions on Microwave Theory and Techniques* **50** 2002) 218–21.
14. N. Zerounian, F. Aniel, B. Barbalat, P. Chevalier, and A. Chantre, *Solid-State Electronics* **53** (2009).
15. J. P. Roux, L. Escotte, R. Plana, J. Graffeuil, S. L. Delage, and H. Blanck, *Transactions on Microwave Theory and Techniques* **43** (1995).
16. L. Escotte, J. P. Roux, R. Plana, J. Graffeuil and A. Gruhle, *IEEE Trans. on Elec. Dev.* **42** (1995).
17. B. Barbalat *et al*., "*Deep trench isolation effect on self-heating of SiGeC HBTs*," (Proc. 35th European Solid-State Device Research Conference, Grenoble, France, September 2005).
18. M. Abboun *et al*., "*Self-heating in InP DHBT technology for 40 Gbit/s ICs*," (Proc. of the 32th European Solid State Device Research Conference, Firenze Italy, September 2002).
19. R. J. Hawkins, *Solid State Electronics* **20** (1977).
20. R. A. Pucel and U. L. Rohde, *IEEE Microwave and Guided Dev. Lett.* **3** (1993).